

Neural Network and Statistical Study of the ^{208}Tl and the ^{214}Bi decay events in SNO

X.Chen,Oxford University

SNO-STR-96-004

February 13, 1996

Abstract

Major radioactivity backgrounds in SNO come from ^{208}Tl decay events in the Thorium chain and ^{214}Bi decay events in the Uranium chain. A neural network and the Chi Square method have been used to statistically distinguish between 6 background event classes : ^{208}Tl and ^{214}Bi in the D_2O , Acrylic Vessel and H_2O . It is possible to determine the number of CC and NC background events without the assumption of the equilibrium in the Thorium and Uranium decay chains. Some results are presented here.

1 Introduction

The neural network pattern recognition technique has been used in many modern physics experiments[1,2,3] including SNO [4]. The ^{208}Tl and the ^{214}Bi decay events in D_2O can be distinguished and their relative ratio can be decided to the satisfying level(error lies

within 10%). Between 30 and 40 nhits, the ^{208}Tl and the ^{214}Bi background are the only major events(see table 3 and 5). Major CC backgrounds come from the ^{208}Tl and the ^{214}Bi decay and most of NC backgrounds come from the free neutrons produced by the high energy gamma rays which are the products of the ^{208}Tl and ^{214}Bi decay. So if we can distinguish 6 event classes (the ^{208}Tl and the ^{214}Bi decay events in D_2O , acrylic vessel and H_2O) simultaneously, the number of these decay events per year can be deduced and hence the number of major CC and NC background events can be determined without the assumption of the secular equilibrium in the Thorium and Uranium decay chains. The neural network technique and chi square fit have been used to accomplish this object. Section 2 describes the constituents of network and the analysis of input parameters to the network. Section 3 is about the result of the neural network to distinguish 6 event classes. Statistical fit result is presented in section 4. The discussion of possible improvements to the performance of the neural network is presented in section 5 . Robustness of neural network is discussed in section 6. Usage of a true calibration source is discussed in section 7.

2 Constituent of the Neural Network

The feed forward and error backpropagation neural network has been proved to be able to accomplish complex pattern recognition tasks. The basic idea of this technology can be found in [6].The network used here is made up of 3 layers : the input layer, the hidden layer and the output layer.

The input layer consists of 20 input units corresponding to the 20 input parameters .These parameters should be chosen to be able to reflect the idiosyncrasy of the different

patterns. They are defined as below:

- Nhits parameter.

Nhits parameter is chosen to reflect the energy spectrum difference between the different event class. For example, see figure 1 : the nhits plot of the ^{208}Tl decay events in D_2O , acrylic vessel and H_2O . At high nhits, the number of the ^{208}Tl decay events in D_2O is smaller than those in H_2O . The number of the ^{208}Tl decay events in Acrylic vessel is between them. At low nhits, the rank is reversed. This can be explained. In order to produce large nhits, the decay products should go outwards the detector rather than go inward because the number of Cerenkov photons produced in the forward hemisphere is much larger than those produced in the backward hemisphere and the photons travelling outwards pass shorter distance before they are detected. The outgoing ^{208}Tl decay products in H_2O produce more PMT hits than those in D_2O because Cerenkov photons produced in D_2O travel longer distance and have to pass through the acrylic vessel, so more likely to be absorbed.

- rfit parameter

definition:

$$par = \frac{(r_{fit} - r_{min})}{(r_{max} - r_{min})}$$

r_{fit} is the distance from the fitted vertex to the center of the detector. r_{min} and r_{max} are the minimal and maximal r_{fit} cut. So this parameter ranges from 0 to 1.

The reason to choose this parameter is obvious : the event reconstructed at the center of the detector is much more likely to be a decay event in D_2O than in the acrylic vessel and H_2O . Figure 2 is the rfit distribution of the ^{208}Tl decay events

in the different regions .Figure 3 is the rfit distribution for the ^{214}Bi decay events .
The difference is obvious.

- θ_{ij} parameters

θ_{ij} is the angle between the i^{th} hitted PMT and the j^{th} hitted PMT ,taking the fitted vertex as the common origin.

definition:

$$\text{par}(k) = \frac{\text{number of } \theta_{ij} \text{ which are less than } \frac{k*\theta_c}{4}}{\text{total number of } \theta_{ij}}$$

k ranges from 1 to 9. θ_c is the cerenkov angle. So $\frac{9}{4} * \theta_c$ is approximately equal to 180 degree.

These parameters are used to distinguish the ^{208}Tl and ^{214}Bi decay events in the same region. Above 30 nhits ,the ^{214}Bi decay events are mostly single electron (3.27 Mev) whereas the ^{208}Tl decay events are always one 2.6145 Mev gamma + an electron + one or more lower energy gamma. This makes the signals of the ^{208}Tl decay events more isotropical than those of the ^{214}Bi decay events. As figure 4 shows , the number of entries of the ^{208}Tl decay events is smaller than those of the ^{214}Bi decay events when θ_{ij} is small ,but larger when θ_{ij} is large. The same situation holds for the ^{208}Tl and ^{214}Bi decay events in H_2O and acrylic vessel.

The advantages of these parameters are that they are rotational invariants and are independent of the fitted event direction which often bring in more errors.

The other way to describe θ_{ij} is the usage of the harmonic parameters [9]. These parameters have been used but did not produce significant difference .

- θ_{ir} parameters

θ_{ir} is the angle between two vectors : one vector is from the fitted vertex to the i^{th} hit PMT, the other one is from the center of the detector to the fitted vertex(radial direction).

definition :

$$par(k) = \frac{\text{number of } \theta_{ir} \text{ which is less than } \frac{k*\pi}{9}}{\text{total number of the pmt hits}}$$

k is from 1 to 9.

These parameters are used to distinguish the same type of event(^{208}Tl or ^{214}Bi decay) in different regions. See Figure 5. The difference between three θ_{ir} distributions can be explained. For the ^{208}Tl decay events in D_2O , the outgoing cerenkov photon is more likely to make a PMT hit than the ingoing one, so the number of entries in small θ_{ir} is relatively large than those in large θ_{ir} , making a relatively smooth peak. For the ^{208}Tl decay events in the acrylic vessel, the cerenkov light travelling along the vessel (normal to the radial direction) is much more likely to be absorbed, so there is a deep valley around 90 degree($\pi/2$). For the ^{208}Tl decay events in H_2O , the cerenkov photons travelling inwards to pass the acrylic vessel has the least probability to hit the pmt. So there is also a deep valley but this time around some θ_{ir} which is larger than that of the acrylic vessel event. The same thing happened in the ^{214}Bi decay event(figure 6).

The hidden layer is made up of 18 units. The output layer is made up of 6 output units, each one representing one type of event class.

3 Neural Network Study

The training and testing procedures in the neural network have been described in a previous paper[5]. The only different thing is now the number of event classes to be distinguished increases to six. So the distinguishing rule here is : If one certain output is highest among the six outputs , then the neural network decides the event belongs to the certain event class corresponding to this output.

In order to get some confidence from neural network , two studies with different cuts have been carried out. The results are presented below :

The first study :

- cut :

$$30 < nhits < 40 , 0 \leq r_{fit} \leq 640$$

These cuts are used to make the number of 6 types of events reconstructed within this window roughly in the same order.

- training set: 6 * 2571, corresponding to 2 types of events in 3 regions. testing set: 6 * 2104
- result : see table 1. Percentage correct = (45.4 +/- 0.4)% .

The second study :

- cut :

$$30 < nhits < 40 , 550 \leq r_{fit} \leq 650$$

These cuts are used to make the number of 6 types of events reconstructed within this window roughly in the same order.

- training set: 6 * 2100, corresponding to 2 types of events in 3 regions. testing set: 6 * 1600
- result : see table 1. Percentage correct = (32.8 +/- 0.5)% .

As we can see from above, neural network can distinguish 6 event classes to some level (45.4% and 32.8% are larger than 1/6) . But this is not the most important thing. There is no need to distinguish 6 event classes event by event . The crucial thing is to distinguish them statistically i.e. to decide the relative ratio between the number of 6 event classes. By this way we can deduce the number of six types of decay events per year , then determine the number of CC and NC background events per year without the assumption of the secular equilibrium in the ^{232}Th and ^{238}U decay chains.

4 Statistical Study

The procedures of calibration and statistical fit are same as the previous paper[5]. Anneal-Amoeba and Levenberg-Marquardt method are used to minimize the following function

:

$$\chi^2 = \sum_i \frac{(d_i - (1 - \sum_k a_k) f_{6i} - \sum_k a_k f_{ki})^2}{\sigma_{d_i}^2 + (1 - \sum_k a_k)^2 \sigma_{f_{6i}}^2 + \sum_k a_k^2 \sigma_{f_{ki}}^2}$$

k is from 1 to 5. i is the bin number. d_i is the normalized data distribution value in the i^{th} bin . f_{ki} is the normalized k^{th} calibration distribution value in the i^{th} bin.

$$\sigma_{d_i}^2 = \frac{d_i}{N}$$

(N is the total number of data events)

$$\sigma_{f_{ki}}^2 = \frac{f_{ki}}{N_k}$$

(N_k is the total number of the k^{th} calibration events)

In a word, it is just trying to fit a mixed data distribution with a linear combination of six calibration distributions in five dimensions space(it can be proved[8] with enough data , the sum of 6 outputs equals to 1.)

As the previous section, two cut studies have been carried out,the result is as below :

The first study :

- cut :

$$30 < nhits < 40 , 0 \leq r_{fit} \leq 640$$

- Number of events reconstructed inside this window per year ,see table 3.
- Results.See table 4.1-4.7

The second study :

- cut :

$$30 < nhits < 40 , 550 \leq r_{fit} \leq 650$$

- Number of events reconstructed inside this window per year ,see table 5.
- Results.See table 6.1-6.6

As we can see from above, the results of chi square fit almost all lie within the statistical error of the true values. So the combination of the neural network technique and chi square fit can decide the ratio between six event classes to the satisfying level. It is possible to deduce the number of six types of decay events per year and the number of CC and NC background per year.

5 Possible Ways of Improving Performance of Neural Network

Temporal information has been considered to be important to describe the pattern in case of noise[7]. Time information has been included ,by adding another parameter t_{ipmt} (the time of the i^{th} hit) ,to distinguish the ^{208}Tl and ^{214}Bi events in D_2O . The result is not significantly better. Maybe it is due to relatively worse fitting accuracy of the background event,so all hits look more like noise. But temporal information should be useful when distinguishing events in different regions because cerenkov photons produced in different regions travel for different length of time to hit the pmt.This is a possible way to improve the performance of the neural network.

The number of hidden layers and hidden nodes did not have significant effects on the performance of the neural network . This has been checked by adding a hidden layer , adding 1 hidden node or subtracting 6 hidden nodes.

The statistical errors in the above results are large. Obviously several thousand events are not enough to describe a distribution in 5 dimensions space.In practice , when the number of events was decreased by a factor of 2 , the performance of the neural network became much worse. So increasing the number of training ,testing and calibration events can improve the performance of the neural network.

6 Robustness of Neural network

Up to now, the calibration set can only come from Monte Carlo. If Monte Carlo can not show the truth accurately or something changes systematically from day to day inside

the detector(eg: the scattering coefficient of Cerenkov photons in D_2O), it is doubtful whether the neural network and chi square fit still give us correct results. So the robustness of the neural network should be checked.

If one increases the isothermal compressibility of both H_2O and D_2O by 20% of their normal values, it increases the amount of Rayleigh scattering by a factor of 1.2.(It is claimed that the overall level of scattering in the detector will be known to be within 10% with a laserball calibration[8]. So increasing the isothermal compressibility by a factor of 10 in the previous paper is inappropriate.) A testing set (6*2467 events for 6 event classes respectively) generated with the increased isothermal compressibility is fed through the originated trained network. The result is as table 7. The result percentage correct is 45.6% . But as discussed in the previous paper , the chi square fit is much more sensitive to the systematical changes than the neural network. So the statistical results should be checked.

Repeat the procedure in the fourth section with the mixed data distribution generated with the the increased isothermal compressibility . The result is as table 8.1-8.6 . As we can see , chi square fit still get a good result (error within 10%).

Another important thing is about the effects on the neural network results by the impurity of the fitted window . It is easy to get rid of the other background events except the ^{208}Tl and ^{214}Bi decay events by simply increasing the nhits threshold of the window. But if using some calibration sources to generate the training and calibration distributions for 6 event classes, there are impurities from the other 5 event classes (ie: sometimes the neural network is taught that the decay events in D_2O or H_2O are from the acrylic vessel.) Six training sets with 10% impurity (ie: 10% events come from the other 5 types of events) are used to train the network and then the network is tested

with the normal testing sets. The result is shown in table 9. The percentage correct is 44.3%. The statistical results are shown in table 10.1-10.7. As tables show , in this case the results are worse, but still lie within the error of the chi square fitting.

The neural network is robust against the modest systematical changes inside the detector and the impurity of the fitted window.

7 Calibration Source

Obviously true calibration is very important, it will give you the confidence of the result of the neural network. For example , ^{220}Rn in Thorium chain and ^{222}Rn in Uranium chain could be used as the calibration sources . They exist as gas which may be easily extracted from Thorium and Uranium. The half life of ^{222}Rn is 3.82 days and the half life of ^{212}Pb which is the decay product of ^{220}Rn is 10.6 hours. So it would in principle not leave any radioactivity inside the detector. ^{222}Rn and ^{220}Rn gas can be added in the detector to produce the training and calibration sets for the decay events in D_2O and H_2O .

For example , in order to get $3 * 5000$ ^{208}Tl decay events in D_2O within the window ($30 < nhits < 40$, $0 < rfit < 640$) for training ,testing and calibration respectively, 262000 ^{208}Tl decay events in D_2O are needed. Among the decay products of ^{220}Rn , ^{212}Pb has the longest half decay lifetime(10.6 hours). Ignoring the other decay time ,

$$\frac{262000}{x} = 1 - e^{-\frac{2.24 * 0.693}{10.6}}$$

$$x = 760478$$

x is the number of ^{212}Pb atoms needed to produce enough ^{208}Tl decay events in two days. It means 760478 ^{220}Rn atoms will produce enough events in two days for the neural network studying.

Assuming equilibrium,

$$\frac{\frac{y}{232} * 6.02 * 10^{23}}{\frac{1.4 * 10^{10}}{0.693} * 365 * 24} = 760478$$

$$y=0.52(\text{gm})$$

y is the mass of Thorium needed to produce enough ^{222}Rn atoms in 1 hour.

The normal ^{212}Pb concentration level in the detector :

$$\frac{z}{\frac{10.6}{0.693}} = \frac{505890}{365 * 24 * 0.36}$$

$$z=161$$

z is the number of ^{212}Pb atoms in the normal detector. The number of ^{208}Tl decay events is taken from [5], considering only 36% of the ^{212}Pb decays proceed to ^{208}Tl .

$$760478 * e^{-9} = 91$$

$$9 * \frac{10.6}{0.693} = 138(\text{hours}) = 5.74(\text{days})$$

So after 5.74 days , only 91 out of 760478 ^{212}Pb atoms remain in the detector compared to 161 ^{212}Pb atoms in the normal detector.

Repeat the calculation for the other 3 types of events , the results are presented in table 11.1 and 11.2 .

8 Conclusion

The neural network plus chi square fit can distinguish the ^{208}Tl and ^{214}Bi decay events in D_2O , acrylic vessel and H_2O . So it is possible to deduce the number of these decay events and hence determine the number of charged and neutral current background events

without assuming the secular equilibrium of the decay chains. These techniques are robust against the modest systematic changes in the detector and the impurity of the fitted window.

References

- [1] The DELPHI Collaboration. *Classification of the hadronic decays of the Z^0 into b and c quark pairs using a neural network* (Physics Letters B,295:383-395,1992)
- [2] Bruce Denby, *Tutorial on neural network applications in high energy physics :1992 perspective.* (Proceedings of the Second International Workshop on Software Engineering,Artificial Intelligence,and Expert Systems for High Energy and Nuclear Physics,page 287-325,La Londe Les Maures,France,1992)
- [3]. Carsten Peterson *Pattern recognition in high energy physics with neural networks.* (L.Cifarelli,editor,QCD at 200Tev,pages 149-163,1992)
- [4] S.Brice *An overview of the Feedforward Neural Network Technique and its application to SNO event Classification*
- [5] X.Chen *A Monte carlo Study of Beta-Gamma Backgrounds from ^{208}Tl and ^{214}Bi* (SNO-STR-96-003)
- [6] John Hertz,Anders Krogh and Richard G.Palmer *Introduction To the Theory of Neural Computation.*
- [7] D.W.Dong, Y.Chan *Neural Network for Recognizing Cerenkov Radiation Patterns*

- [8] H.Gish *A probabilistic approach to the understanding and training of neural network classifiers.* (Proceedings of the 1990 IEEE International Conference on Acoustic, Speech, and Signal Processing, volume 3, page 1361-1364, April 1990)
- [9] S.Brice *The Results of a Neural Network Statistical Event Class Analysis* (SNO-STR-96-001)

Table Caption

Table 1

Neural network output for 6 event classes with cuts -

$$30 < nhits < 40, 0 \leq r_{fit} \leq 640$$

1. the ^{208}Tl decay events in D_2O ; 2. the ^{214}Bi decay events in D_2O ;
3. the ^{208}Tl decay events in the acrylic vessel ; 4. the ^{214}Bi decay events in the acrylic vessel ;
5. the ^{208}Tl decay events in H_2O ; 6. the ^{214}Bi decay events in H_2O .

The column is the true event class. The row is the decision of the neural network.

Table 2

Neural network output for 6 event classes with cuts -

$$30 < nhits < 40, 550 \leq r_{fit} \leq 650$$

1. the ^{208}Tl decay events in D_2O ; 2. the ^{214}Bi decay events in D_2O ;
3. the ^{208}Tl decay events in the acrylic vessel ; 4. the ^{214}Bi decay events in the acrylic vessel ;
5. the ^{208}Tl decay events in H_2O ; 6. the ^{214}Bi decay events in H_2O .

The column is the true event class. The row is the decision of the neural network.

Table 3

Number of events reconstructed inside the window per year:

$$30 < nhits < 40, 0 \leq r_{rfit} \leq 640$$

Table 4.1-4.7

Statistical study results of the distinguishment of 6 event classes within the window :

$$30 < nhits < 40, 550 \leq r_{rfit} \leq 640$$

1. the ^{208}Tl decay events in D_2O ; 2. the ^{214}Bi decay events in D_2O ;
3. the ^{208}Tl decay events in the acrylic vessel ; 4. the ^{214}Bi decay events in the acrylic vessel ;
5. the ^{208}Tl decay events in H_2O ; 6. the ^{214}Bi decay events in H_2O .

Table 5

Number of events reconstructed inside the window per year:

$$30 < nhits < 40, 550 \leq r_{rfit} \leq 650$$

Table 6.1-6.6

Statistical study results of the distinguishment of 6 event classes within the window :

$$30 < nhits < 40, 550 \leq r_{rfit} \leq 650$$

1. the ^{208}Tl decay events in D_2O ; 2. the ^{214}Bi decay events in D_2O ;
3. the ^{208}Tl decay events in the acrylic vessel ; 4. the ^{214}Bi decay events in the acrylic vessel ;
5. the ^{208}Tl decay events in H_2O ; 6. the ^{214}Bi decay events in H_2O .

Table 7

Systematical study of the neural network(increase the isothermal compressibility of both H_2O and D_2O by 20%. Neural network output for 6 event classes with cuts -

$$30 < nhits < 40, 0 \leq r_{rfit} \leq 640$$

1. the ^{208}Tl decay events in D_2O ; 2. the ^{214}Bi decay events in D_2O ;
3. the ^{208}Tl decay events in the acrylic vessel ; 4. the ^{214}Bi decay events in the acrylic vessel ;
5. the ^{208}Tl decay events in H_2O ; 6. the ^{214}Bi decay events in H_2O .

The row is the true event class. The column is the decision of the neural network.

Table 8.1-8.6

Statistical study results of the distinguishment of 6 event classes within the window when the isothermal compressibility of both H_2O and D_2O are increased by 20%.

$$30 < nhits < 40, 0 \leq r_{rfit} \leq 640$$

1. the ^{208}Tl decay events in D_2O ; 2. the ^{214}Bi decay events in D_2O ;
3. the ^{208}Tl decay events in the acrylic vessel ; 4. the ^{214}Bi decay events in the acrylic vessel ;
5. the ^{208}Tl decay events in H_2O ; 6. the ^{214}Bi decay events in H_2O .

Table 9

Systematical study of the neural network(impurity of the studying window is 10%)
Neural network output for 6 event classes with cuts -

$$30 < nhits < 40, 0 \leq r_{rfit} \leq 640$$

1. the ^{208}Tl decay events in D_2O ; 2. the ^{214}Bi decay events in D_2O ;
3. the ^{208}Tl decay events in the acrylic vessel ; 4. the ^{214}Bi decay events in the acrylic vessel ;
5. the ^{208}Tl decay events in H_2O ; 6. the ^{214}Bi decay events in H_2O .

The row is the true event class. The column is the decision of the neural network.

Table 10.1-10.6

Statistical study results of the distinguishment of 6 event classes within the window when the impurity of the studying window is 20%.

$$30 < nhits < 40, 0 \leq r_{fit} \leq 640$$

1. the ^{208}Tl decay events in D_2O ; 2. the ^{214}Bi decay events in D_2O ;
3. the ^{208}Tl decay events in the acrylic vessel ; 4. the ^{214}Bi decay events in the acrylic vessel ;
5. the ^{208}Tl decay events in H_2O ; 6. the ^{214}Bi decay events in H_2O .

Table 11

Calibration source ^{220}Rn .

1. Number of ^{220}Rn atoms needed to produce $3 * 1500$ ^{208}Tl decay events within the studying window in 2 days.
2. Mass of ^{232}Th needed to produce enough ^{220}Rn atoms in an hour.
3. Number of days needed to get rid of the radioactivity from the calibration ^{220}Rn gas.
4. Impurity of the studying window ($30 < nhits < 40, 0 < r_{fit} < 640$)

Table 11.2

Calibration source ^{222}Rn .

1. Number of ^{222}Rn atoms needed to produce $3 * 1500$ ^{214}Bi decay events within the studying window in 2 days.
2. Mass of ^{238}U needed to produce enough ^{222}Rn atoms in an hour.
3. Number of days needed to get rid of the radioactivity from the calibration ^{222}Rn gas.
4. Impurity of the studying window ($30 < nhits < 40, 0 < rfit < 640$)

Figure Caption

Figure 1

Nhits distributions of 3 event classes. Solid line is for the ^{208}Tl decay events in D_2O , dotted line is for the ^{208}Tl decay events in H_2O , dashed line is for the ^{208}Tl decay events in the acrylic vessel.

Figure 2

R_{fit} parameter distributions for the 3 event classes. Solid line is for the ^{208}Tl decay events in H_2O , dotted line is for the ^{208}Tl decay events in the acrylic vessel, dashed line is for the ^{208}Tl decay events in D_2O .

Figure 3

R_{fit} parameter distributions for the 3 event classes. Solid line is for the ^{214}Bi decay events in H_2O , dotted line is for the ^{214}Bi decay events in D_2O , dashed line is for the ^{214}Bi decay events in the acrylic vessel.

Figure 4

θ_{ij} distributions for two event classes, the solid line for ^{214}Bi decay events in D_2O , dashed line is for the ^{208}Tl decay events in D_2O . Unit is radian.

Figure 5

θ_{ir} distributions for 3 event classes, the solid line for ^{208}Tl decay events in the acrylic vessel, dashed line is for the ^{208}Tl decay events in D_2O , dotted line is for the ^{208}Tl decay events in H_2O . Unit is radian.

Figure 6

θ_{ir} distributions for 3 event classes , the solid line for ^{214}Bi decay events in the acrylic vessel, dashed line is for the ^{214}Bi decay events in H_2O , dotted line is for the ^{214}Bi decay events in D_2O . Unit is radian.

Table 1

		event class decided by neural network					
		1	2	3	4	5	6
true event class	1	850	918	185	64	42	45
	2	394	1403	143	89	20	55
	3	25	110	910	283	303	473
	4	11	85	701	707	143	457
	5	11	43	480	118	741	711
	6	3	33	392	149	411	1116

Percentage Correct = (45.4 +/- 0.4)%

Table 2

		event class decided by neural network					
		1	2	3	4	5	6
true event class	1	576	209	93	290	303	129
	2	358	492	66	328	170	186
	3	314	105	177	497	285	222
	4	169	81	119	842	169	220
	5	299	107	87	256	561	290
	6	195	135	84	359	328	499

Percentage Correct = (32.8 +/- 0.5)%

Table 3

region	Thorium Concentration(g/g)	^{208}Tl decay per year
1000 tons D_2O	$11 * 10^{-15}$	29031
30 tons Acrylic Vessel	$4.6 * 10^{-13}$	35093
8000 tons H_2O	$7.53 * 10^{-14}$	63336
region	Uranium Concentration(g/g)	^{214}Bi decay per year
1000 tons D_2O	$11 * 10^{-15}$	26514
30 tons Acrylic Vessel	$6.3 * 10^{-13}$	13815
8000tons H_2O	$8.6 * 10^{-14}$	82314

other types of events	events per year reconstructed inside the window
Charged Current Events	282 (1/3 SSM level)
Neural Current Events	192 (Full SSM level)
^{228}Ac decay events in D_2O	11 (equilibrium)
^{212}Bi decay events in D_2O	207 (equilibrium)
^{234}Pa decay events in D_2O	1643 (equilibrium)
^{40}K decay events in 2.5 tons MgCl_2	< 426 (1ppm K concentration level in MgCl_2)

Table 4.1

	true event number	true class fraction	decided class fraction
1	2104	0.1667	0.1606 +/- 0.0120
2	2104	0.1667	0.1784 +/- 0.0122
3	2104	0.1667	0.1614 +/- 0.0195
4	2104	0.1667	0.1653 +/- 0.0143
5	2104	0.1667	0.1632 +/- 0.0199
6	2104	0.1667	0.1711 +/- 0.0357

Table 4.2

	true event number	true class fraction	decided class fraction
1	5000	0.277	0.267 +/- 0.014
2	2000	0.111	0.127 +/- 0.013
3	5000	0.277	0.268 +/- 0.018
4	2000	0.111	0.114 +/- 0.012
5	2000	0.111	0.114 +/- 0.017
6	2000	0.111	0.111 +/- 0.033

Table 4.3

	true event number	true class fraction	decided class fraction
1	4000	0.3077	0.2941 +/- 0.0161
2	2000	0.1538	0.1757 +/- 0.0153
3	2000	0.1538	0.1501 +/- 0.0191
4	2000	0.1538	0.1517 +/- 0.0135
5	2000	0.1538	0.1653 +/- 0.0181
6	1000	0.0769	0.0632 +/- 0.0370

Table 4.4

	true event number	true class fraction	decided class fraction
1	1000	0.0909	0.0988 +/- 0.0106
2	2000	0.1818	0.1773 +/- 0.0114
3	3000	0.2727	0.2549 +/- 0.0221
4	2000	0.1818	0.1887 +/- 0.0161
5	1000	0.0909	0.1125 +/- 0.0206
6	2000	0.1818	0.1678 +/- 0.0377

Table 4.5

	true event number	true class fraction	decided class fraction
1	3000	0.2857	0.2791 +/- 0.0160
2	1000	0.0952	0.1099 +/- 0.0147
3	1000	0.0952	0.0879 +/- 0.0220
4	2000	0.1905	0.1945 +/- 0.0160
5	2500	0.2381	0.2467 +/- 0.0219
6	1000	0.0952	0.0818 +/- 0.0410

Table 4.6

	true event number	true class fraction	decided class fraction
1	2000	0.1481	0.1469 +/- 0.0111
2	2000	0.1481	0.1547 +/- 0.0112
3	4000	0.2963	0.2643 +/- 0.0210
4	2000	0.1481	0.1621 +/- 0.0147
5	2000	0.1481	0.1649 +/- 0.0206
6	1500	0.1111	0.1072 +/- 0.0365

Table 4.7

	true event number	true class fraction	decided class fraction
1	600	0.0909	0.0962 +/- 0.0109
2	600	0.0909	0.0920 +/- 0.0108
3	900	0.1364	0.1232 +/- 0.0249
4	300	0.0455	0.0574 +/- 0.0146
5	1800	0.2727	0.2644 +/- 0.0330
6	2400	0.3636	0.3669 +/- 0.0464

Table 5

region	Thorium Concentration(g/g)	^{208}Tl decay per year
1000 tons D_2O	$11 * 10^{-15}$	7567
30 tons Acrylic Vessel	$4.6 * 10^{-13}$	36913
8000 tons H_2O	$7.53 * 10^{-14}$	83200
region	Uranium Concentration(g/g)	^{214}Bi decay per year
1000 tons D_2O	$11 * 10^{-15}$	6804
30 tons Acrylic Vessel	$6.3 * 10^{-13}$	13995
8000tons H_2O	$8.6 * 10^{-14}$	15547

other types of events	events per year reconstructed inside the window
Charged Current Events	73 (1/3 SSM level)
Neural Current Events	44 (Full SSM level)
^{228}Ac decay events in D_2O	6 (equilibrium)
^{212}Bi decay events in D_2O	46 (equilibrium)
^{234}Pa decay events in D_2O	491 (equilibrium)
^{40}K decay events in 2.5 tons MgCl_2	< 426 (1ppm K concentration level in MgCl_2)

Table 6.1

	true event number	true class fraction	decided class fraction
1	1000	0.1666	0.1828 +/- 0.0477
2	1000	0.1666	0.1441 +/- 0.0275
3	1000	0.1666	0.1867 +/- 0.0516
4	1000	0.1666	0.1734 +/- 0.0249
5	1000	0.1666	0.1446 +/- 0.0396
6	1000	0.1666	0.1684 +/- 0.0887

Table 6.2

	true event number	true class fraction	decided class fraction
1	1000	0.1111	0.1023 +/- 0.0419
2	1000	0.1111	0.1188 +/- 0.0231
3	3000	0.3333	0.3567 +/- 0.0437
4	1000	0.1111	0.1078 +/- 0.0195
5	2000	0.2222	0.2179 +/- 0.0357
6	1000	0.1111	0.0965 +/- 0.0765

Table 6.3

	true event number	true class fraction	decided class fraction
1	1500	0.107	0.0833 +/- 0.0369
2	1500	0.107	0.1179 +/- 0.0202
3	6000	0.428	0.4577 +/- 0.0365
4	1000	0.0714	0.0694 +/- 0.0151
5	3000	0.214	0.2193 +/- 0.0310
6	1000	0.0714	0.0525 +/- 0.0655

Table 6.4

	true event number	true class fraction	decided class fraction
1	300	0.0455	0.0696 +/- 0.0478
2	300	0.0455	0.0247 +/- 0.0240
3	1500	0.227	0.2564 +/- 0.0506
4	750	0.114	0.1037 +/- 0.0198
5	3000	0.454	0.4044 +/- 0.0451
6	750	0.114	0.1414 +/- 0.0886

Table 6.5

	true event number	true class fraction	decided class fraction
1	1000	0.0952	0.0872 +/- 0.0405
2	1500	0.1428	0.1427 +/- 0.0227
3	3000	0.2857	0.3203 +/- 0.0402
4	1000	0.0952	0.0880 +/- 0.0169
5	3000	0.2857	0.2775 +/- 0.0358
6	1000	0.0952	0.0843 +/- 0.0730

Table 6.6

	true event number	true class fraction	decided class fraction
1	1000	0.0909	0.0839 +/- 0.0409
2	1000	0.0909	0.0967 +/- 0.0216
3	4000	0.3636	0.3814 +/- 0.0417
4	1000	0.0909	0.0922 +/- 0.0177
5	3000	0.2727	0.2720 +/- 0.0364
6	1000	0.0909	0.0738 +/- 0.0742

Table 7

		event class decided by neural network					
		1	2	3	4	5	6
true event class	1	994	1080	185	94	38	76
	2	438	1644	161	131	17	76
	3	64	100	902	394	313	694
	4	29	74	564	991	150	659
	5	25	34	456	184	751	1017
	6	12	26	338	212	418	1461

Percentage Correct = (45.6 +/- 0.4)%

Table 8.1

	true event number	true class fraction	decided class fraction
1	2467	0.1667	0.1711 +/- 0.0122
2	2467	0.1667	0.1560 +/- 0.0119
3	2467	0.1667	0.1709 +/- 0.0208
4	2467	0.1670	0.1653 +/- 0.0144
5	2467	0.1741	0.1632 +/- 0.0207
6	2467	0.1580	0.1711 +/- 0.0369

Table 8.2

	true event number	true class fraction	decided class fraction
1	5000	0.277	0.2836 +/- 0.0150
2	2000	0.111	0.1039 +/- 0.0136
3	5000	0.277	0.2509 +/- 0.0202
4	2000	0.111	0.1310 +/- 0.0131
5	2000	0.111	0.1324 +/- 0.0180
6	2000	0.111	0.0982 +/- 0.0362

Table 8.3

	true event number	true class fraction	decided class fraction
1	4000	0.3077	0.3193 +/- 0.0175
2	2000	0.1538	0.1391 +/- 0.0162
3	2000	0.1538	0.1477 +/- 0.0214
4	2000	0.1538	0.1649 +/- 0.0149
5	2000	0.1538	0.1614 +/- 0.0191
6	1000	0.0769	0.0678 +/- 0.0402

Table 8.4

	true event number	true class fraction	decided class fraction
1	1000	0.0909	0.1030 +/- 0.0109
2	2000	0.1818	0.1603 +/- 0.0112
3	3000	0.2727	0.2781 +/- 0.0243
4	2000	0.1818	0.1886 +/- 0.0171
5	1000	0.0909	0.1039 +/- 0.0217
6	2000	0.1818	0.1661 +/- 0.0400

Table 8.5

	true event number	true class fraction	decided class fraction
1	2000	0.1481	0.1548 +/- 0.0116
2	2000	0.1481	0.1346 +/- 0.0112
3	4000	0.2963	0.2934 +/- 0.0231
4	2000	0.1481	0.1624 +/- 0.0155
5	2000	0.1481	0.1610 +/- 0.0215
6	1500	0.1111	0.0939 +/- 0.0387

Table 8.6

	true event number	true class fraction	decided class fraction
1	600	0.0909	0.0938 +/- 0.0108
2	600	0.0909	0.0805 +/- 0.0105
3	900	0.1364	0.1369 +/- 0.0246
4	300	0.0455	0.0465 +/- 0.0140
5	1800	0.2727	0.2767 +/- 0.0330
6	2400	0.3636	0.3656 +/- 0.0460

Table 9

		event class decided by neural network					
		1	2	3	4	5	6
true event class	1	908	743	258	53	22	16
	2	447	1225	213	74	9	32
	3	31	65	1264	269	144	227
	4	18	65	971	675	56	215
	5	14	35	895	133	492	431
	6	4	28	746	192	284	746

Percentage Correct = (44.3 +/- 0.5)%

Table 10.1

	true event number	true class fraction	decided class fraction
1	2000	0.1667	0.1739 +/- 0.0154
2	2000	0.1667	0.1705 +/- 0.0151
3	2000	0.1667	0.1377 +/- 0.0248
4	2000	0.1667	0.1691 +/- 0.0173
5	2000	0.1667	0.1478 +/- 0.0242
6	2000	0.1667	0.2011 +/- 0.0444

Table 10.2

	true event number	true class fraction	decided class fraction
1	5000	0.277	0.2998 +/- 0.0176
2	2000	0.111	0.1100 +/- 0.0158
3	5000	0.277	0.2387 +/- 0.0220
4	2000	0.111	0.1231 +/- 0.0141
5	2000	0.111	0.1101 +/- 0.0206
6	2000	0.111	0.1184 +/- 0.0408

Table 10.3

	true event number	true class fraction	decided class fraction
1	4000	0.3077	0.3364 +/- 0.0206
2	2000	0.1538	0.1576 +/- 0.0190
3	2000	0.1538	0.1305 +/- 0.0245
4	2000	0.1538	0.1548 +/- 0.0165
5	2000	0.1538	0.1347 +/- 0.0223
6	1000	0.0769	0.0860 +/- 0.0464

Table 10.4

	true event number	true class fraction	decided class fraction
1	1000	0.0909	0.0948 +/- 0.0137
2	2000	0.1818	0.1779 +/- 0.0142
3	3000	0.2727	0.2536 +/- 0.0273
4	2000	0.1818	0.1856 +/- 0.0191
5	1000	0.0909	0.0763 +/- 0.0261
6	2000	0.1818	0.2120 +/- 0.0467

Table 10.5

	true event number	true class fraction	decided class fraction
1	3000	0.2857	0.3114 +/- 0.0202
2	1000	0.0952	0.0919 +/- 0.0182
3	1000	0.0952	0.0749 +/- 0.0271
4	2000	0.1905	0.1940 +/- 0.0189
5	2500	0.2381	0.2285 +/- 0.0262
6	1000	0.0952	0.0994 +/- 0.0502

Table 10.6

	true event number	true class fraction	decided class fraction
1	2000	0.1481	0.1493 +/- 0.0139
2	2000	0.1481	0.1517 +/- 0.0136
3	4000	0.2963	0.2767 +/- 0.0247
4	2000	0.1481	0.1570 +/- 0.0167
5	2000	0.1481	0.1349 +/- 0.0239
6	1500	0.1111	0.1304 +/- 0.0429

Table 10.7

	true event number	true class fraction	decided class fraction
1	600	0.0909	0.0901 +/- 0.0138
2	600	0.0909	0.0828 +/- 0.0135
3	900	0.1364	0.1166 +/- 0.0313
4	300	0.0455	0.0327 +/- 0.0208
5	1800	0.2727	0.2550 +/- 0.0394
6	2400	0.3636	0.4229 +/- 0.0578

Table 11.1

	1	2	3	4
D_2O	760478	0.52(gm)	5.74	7.57%
H_2O	$3.5 * 10^6$	4.58(gm)	5.1	6.32%

Table 11.2

	1	2	3	4
D_2O	$8.3 * 10^6$	0.019(gm)	27.6	7.67%
H_2O	$3.1 * 10^7$	0.0091(gm)	22.1	5.62%

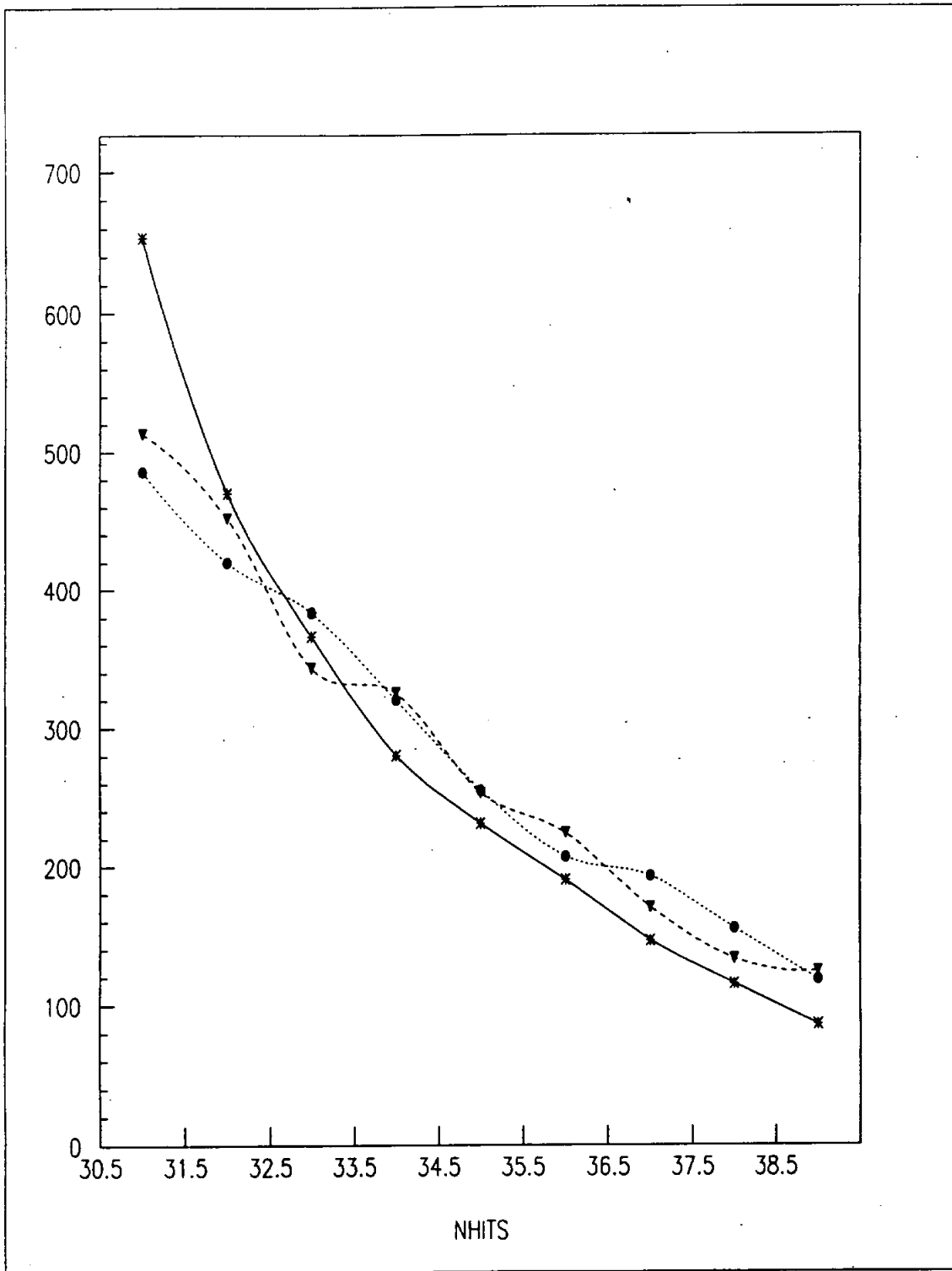


Figure 1: Nhits distribution

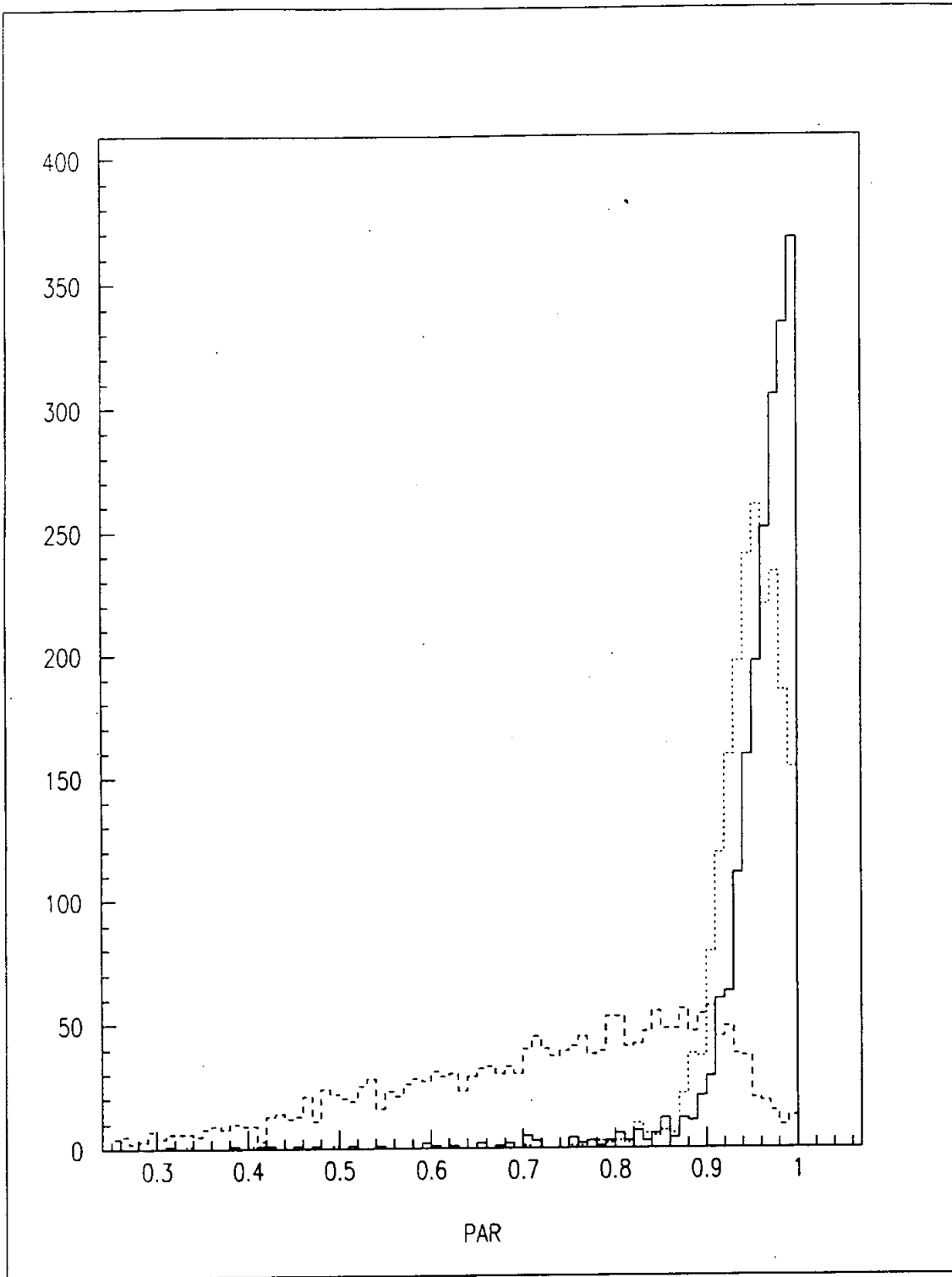


Figure 2: R_{fit} distributions for the ^{208}Tl decay events

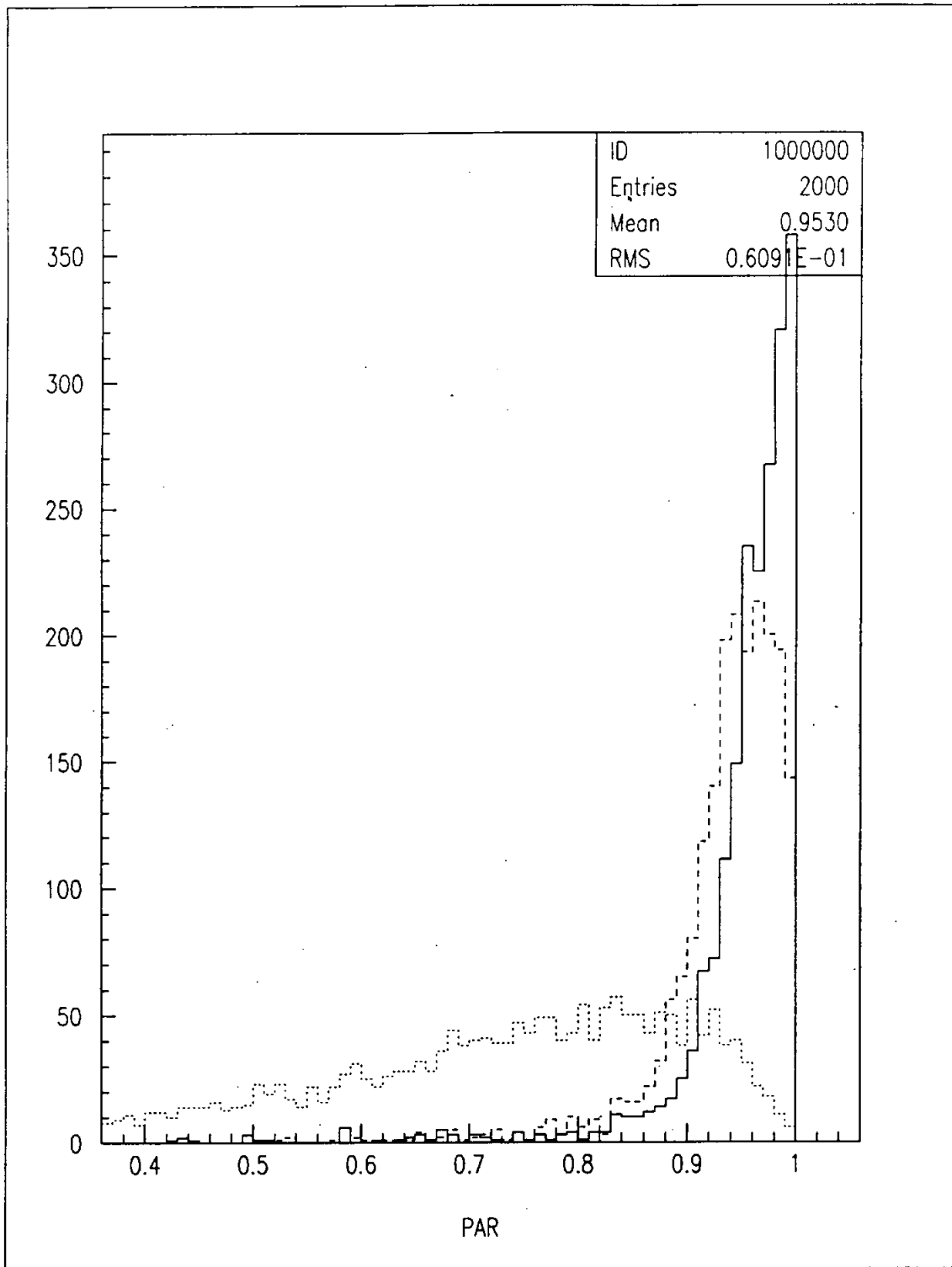


Figure 3: R_{fit} distributions for the ^{214}Bi decay events

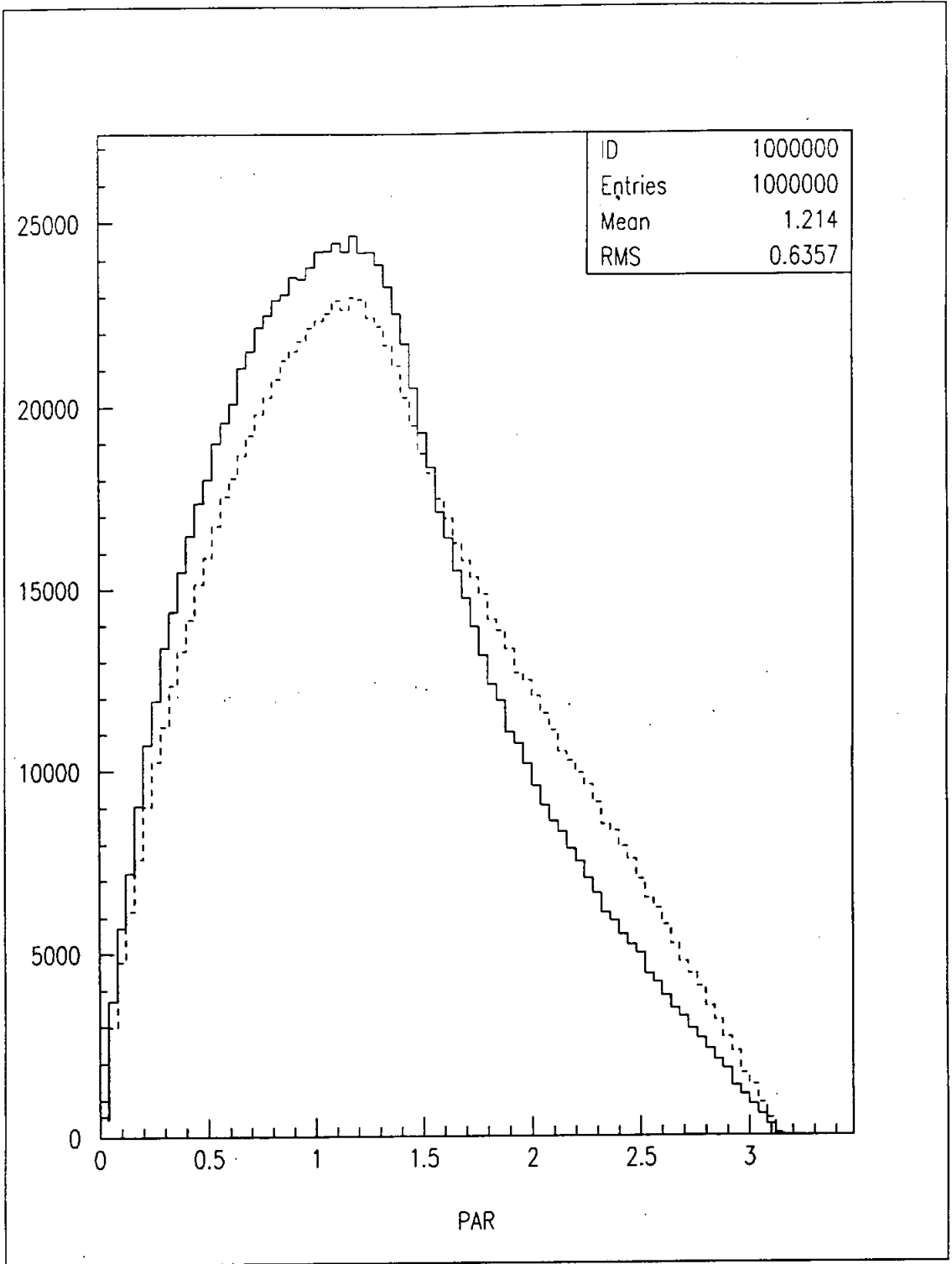


Figure 4: θ_{ij} distributions for the ^{208}Tl and ^{214}Bi decay events in D_2O

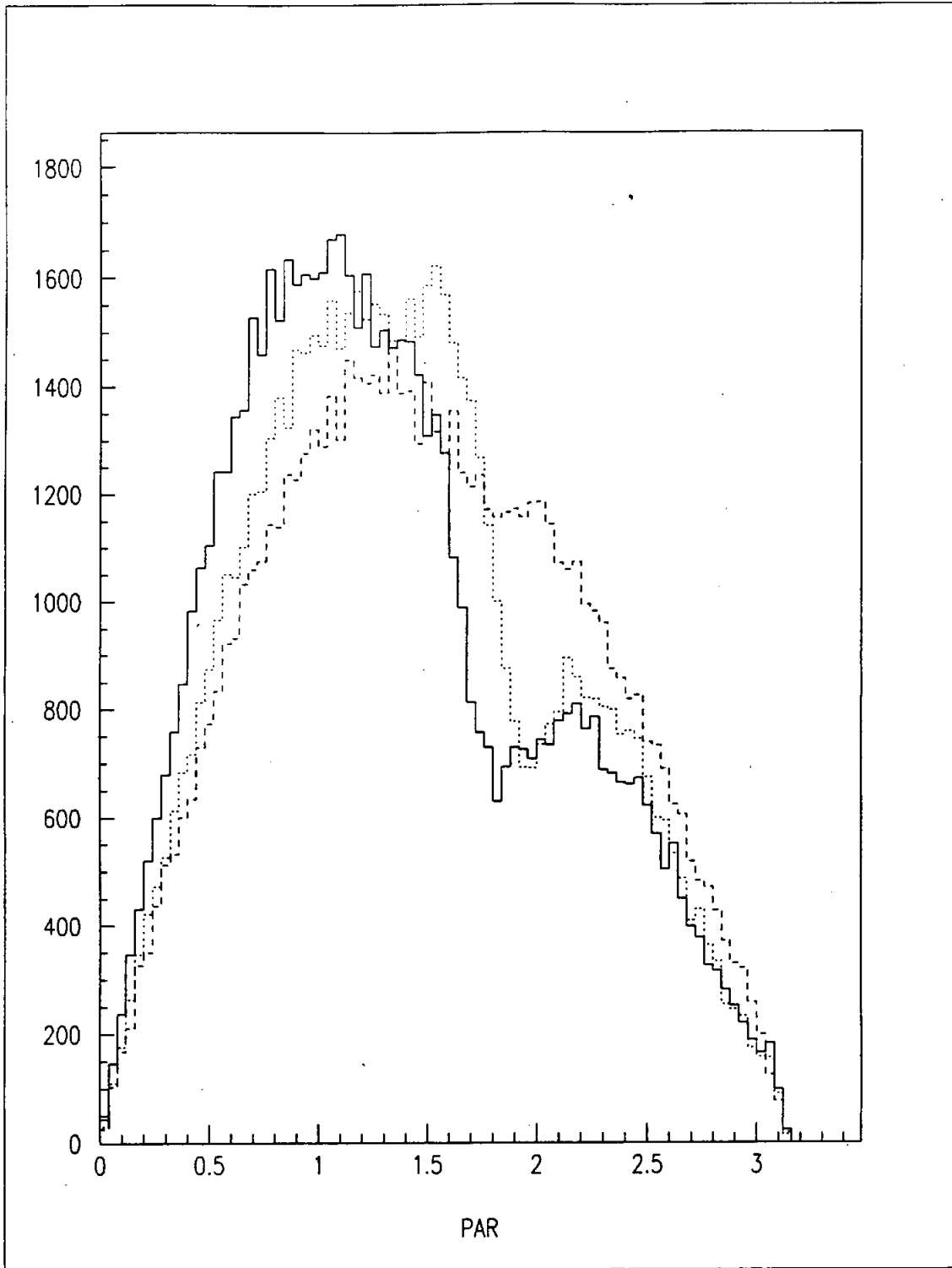


Figure 5: θ_{ir} distribution for the ^{208}Tl decay events in D_2O , acrylic vessel and H_2O .

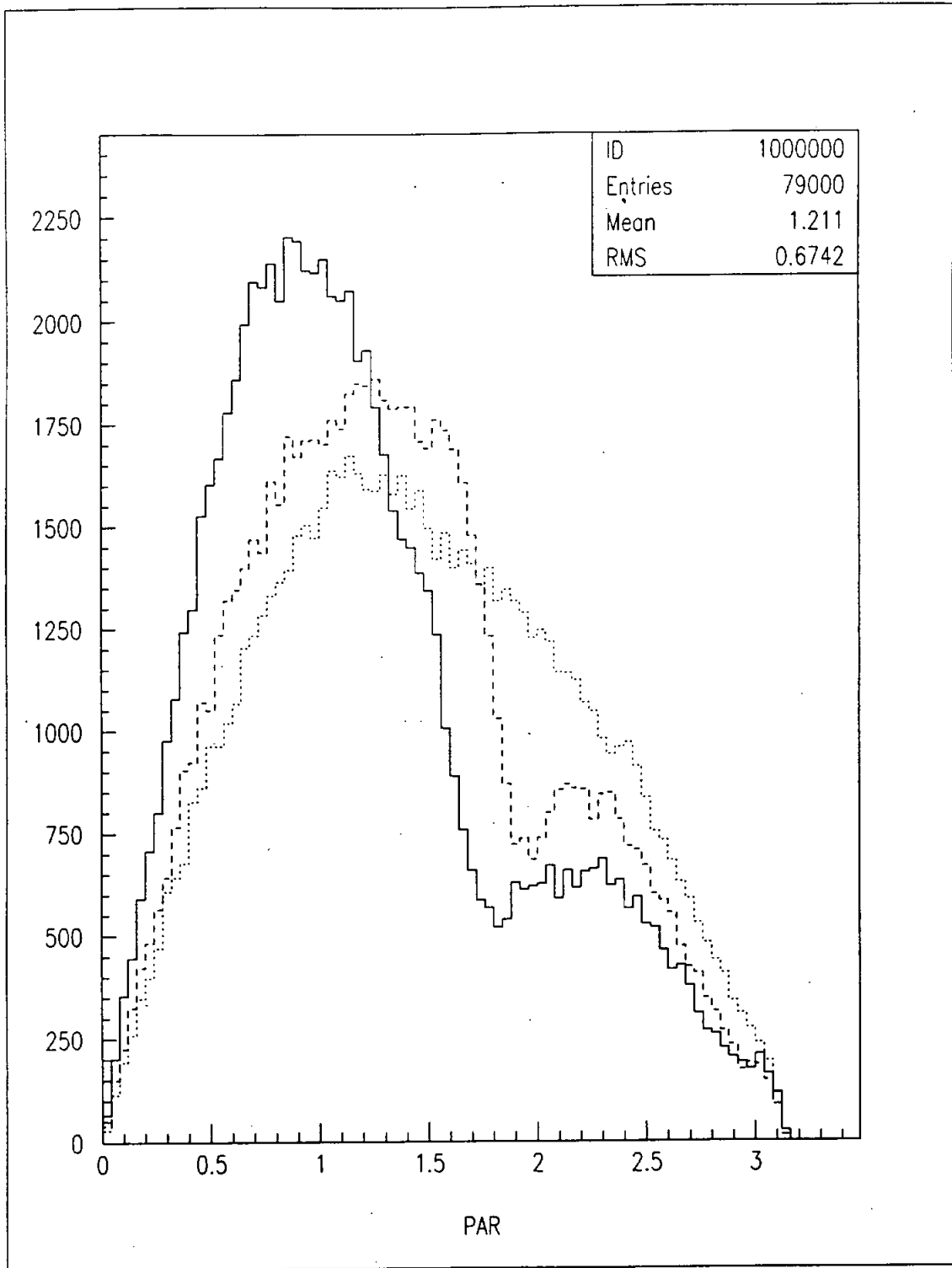


Figure 6: θ_{ir} distribution for the ^{214}Bi decay events in D_2O , acrylic vessel and H_2O .